Hindawi
International Journal of RF and Microwave Computer-Aided Engineering
Volume 2023, Article ID 7871837, 8 pages
https://doi.org/10.1155/2023/7871837

Research Article

A Wide-Angle Scanning Planar Array Based on Four-Mode Pattern-Reconfigurable Elements

Samuel de Jésus Ndimubandi,[1,2] **Xiao Ding**,[1] **and Yu Zeng**[1]

[1]*Institute of Applied Physics, University of Electronic Science and Technology of China, Chengdu 611731, China*
[2]*Yangtze Delta Region Institute (Huzhou), University of Electronic Science and Technology of China, Huzhou 313001, China*

Correspondence should be addressed to Xiao Ding; xding@uestc.edu.cn

Received 27 October 2022; Revised 10 December 2022; Accepted 13 December 2022; Published 8 February 2023

Academic Editor: Jin Xu

This paper presents a design of a wide-angle scanning planar array based on a reconfigurable antenna with four radiation patterns for 5G applications. The pattern-reconfigurable antennas (PRAs), capable of switching into four radiation patterns with the help of PIN diodes, constitute the basic elements of the planar array. By exciting each port individually and combining the scans of the PRAs operating at four symmetrical modes in four quadrant subspaces, the main beam of the proposed scanning planar array can scan subspaces I, II, III, and IV by directing the main lobe from -65° to 65° with side lobes less than -7 dB, while supporting a 3 dB scanning coverage of up to 83.5° for each quadrant in the elevation plane. Due to its compactness, simpler biasing network, and more significant beam-scanning coverage, the scanning array by using four-mode PRAs has better performance, via simulation and measurement result agreement.

1. Introduction

In various applications, such as advanced military and commercial technology, the array antenna is often used owing to its high scanning speed and precision [1–4]. Several wide-angle beam scanning links to phased arrays have been implemented for radar applications, and various kinds of reconfigurable antenna elements for the array have been proposed to improve scanning range and performance [5–9].

Four fundamental approaches for extending the scanner beam coverage have been explored. Firstly, the surface-wave-based antenna array provides wide-angle scanning. Surface waves are often assumed to enhance element coupling. The reference 10 proposes an eight-element linear array of horizontal wire antennas with a high impedance surface (HIS) and a wide beam radiation pattern. The maximum elevation scan angle of the phased array is 85°. Secondly, two types of antennas perform wide-angle scanning using the mirror concept. One antenna parallels an electric current with a magnetic conductor (JpM). Another antenna involves magnetizing an electric conductor (MpE). According to image theory, grounding three sides of the microstrip antenna produces a magnetic current. Theoretically, the phased array antenna composed of JpM or MpE antennas provides excellent scanning performance over the whole upper half of space [11]. Thirdly, the time reversal (TR) method optimizes the wide-angle scanning array by considering coupling [12]. Lastly, with the aid of PIN diodes and combining the scans of PRAs operating in two symmetrical modes in two subspaces, the phased array can scan its beam from -81 to +81 in the elevation plane with a gain fluctuation of less than 3 dB [13]. These approaches can provide wide beam-scanning coverage. Miniaturized patch antennas, less than half-wavelength, are needed to avoid grating lobes while scanning the main beam. In wireless communication, using reconfigurable antenna patterns to increase beamwidth has become increasingly prevalent [14]. The reference 15 shows that a planar end-loaded dipole phased array using PRA components can scan its main beam from -60 to +60. Reference 16 suggested a 4-PRAs linear array. The array scans

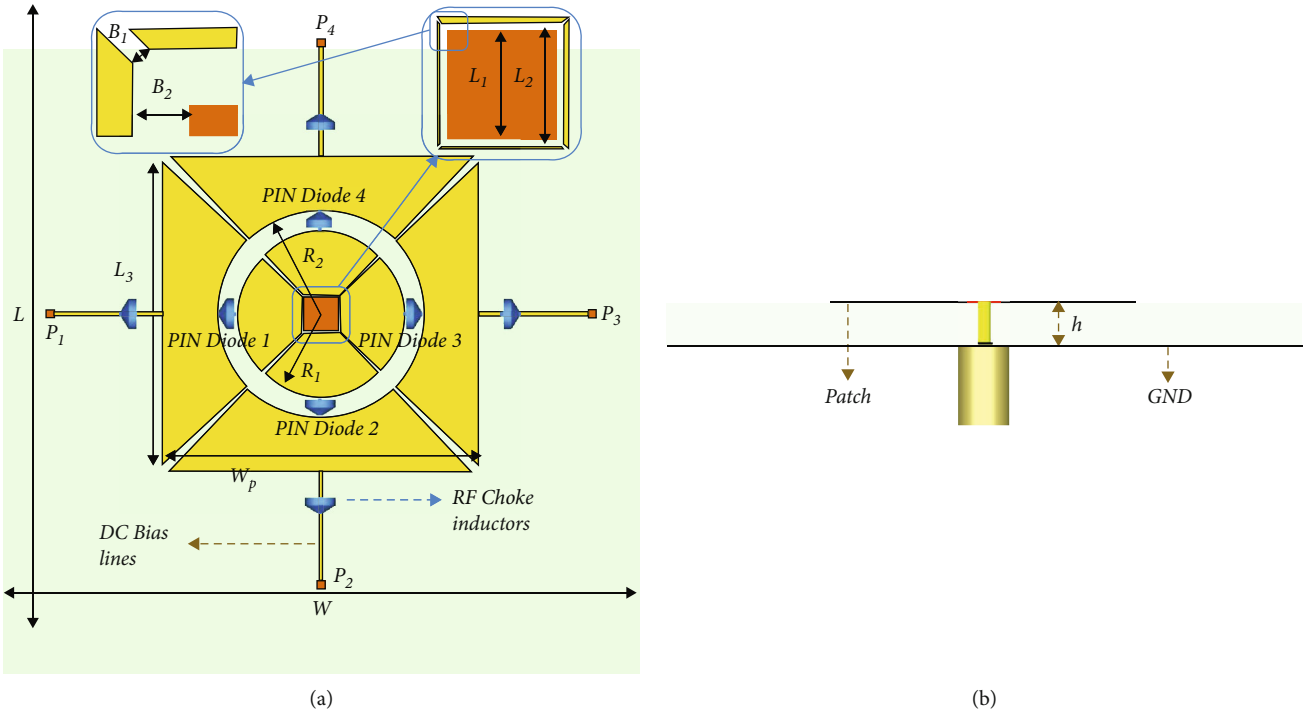

Figure 1: Geometry of the proposed PRA. (a) Top view. (b) Side view.

Table 1: Switch mode configuration.

SS	Mode-1	Mode-2	Mode-3	Mode-4
S_1	ON	OFF	OFF	OFF
S_2	OFF	ON	OFF	OFF
S_3	OFF	OFF	ON	OFF
S_4	OFF	OFF	OFF	ON
BD	0°	90°	180°	270°

SS: switch state; BD: beam direction.

from -70 to +70, with a gain fluctuation of less than 1 dB and a side lobe level (SLL) of less than 11 dB. Using PRA components require a complex biasing network, which make building wide-angle scanning arrays challenging.

This paper proposes four-mode PRA as the basis of scanning planar array elements. PRA has four radiation patterns in its four operational modes and can scan up to 12° in the elevation plane. This design's PRA element consists of four basic PIN diodes on the patch, symmetrical reconfigurable modes, a wide-scanning angle, and a low SLL. In addition, the proposed scanning planar array antenna is compact, simple, and has a better performance. A prototype-scanning array has been developed, fabricated, and tested.

2. PRA Element Design and Analysis

2.1. PRA Element Configuration. The proposed pattern-reconfigurable antenna (PRA) element is a square-shaped microstrip printed on a grounded FR4 substrate (4.4 of permittivity, 0.025 of loss tangent, and 2 mm of thickness), as shown in Figure 1. The proposed square-shaped microstrip has four main sections. The initial section is a 50-coaxial cable-powered patch with a minimized square form placed in the center of the patch. Four trapezoid-shaped cells are positioned symmetrically around the powered square slot. Each trapezoid-shaped cell is divided by an annular slot to generate the second section as a rounded trapezoid-shaped coupling cell and the third as a curved trapezoid-shaped radiation cell. The fourth section consists of four 1 mm long PIN diode switches that connect or disconnect the coupling cells and radiation cells, therefore altering the radiation structure.

When the switch shifts to the ON mode, the radiation cell attached to the associated coupling cell is activated. The radiation cell will no longer function when the switch is in the OFF mode. The proposed PRA operates in four radiation modes by manipulating the switch states. The radius of the annular and base of the trapezoid-shaped slits variation is used to achieve impedance matching of the antenna and to gain the radiation pattern reconfigurable features by controlling the four distinct switch modes. The base of the trapezoid-shaped slit is between the trapezoid-shaped cells from the limit of the inner square to the outer square corner. The overall dimensions are $0.525\lambda \times 0.525\lambda$, and the total thickness is 2.07 mm. The proposed PRA is designed and simulated using CST STUDIO 2020.

2.2. PIN Diode Switch and Bias Circuit. The proposed PRA incorporates four PIN diode switches for the four modes as current-controlled resistors at RF and microwave frequencies with resistances fixed from 1 Ω for the ON to 100 kΩ

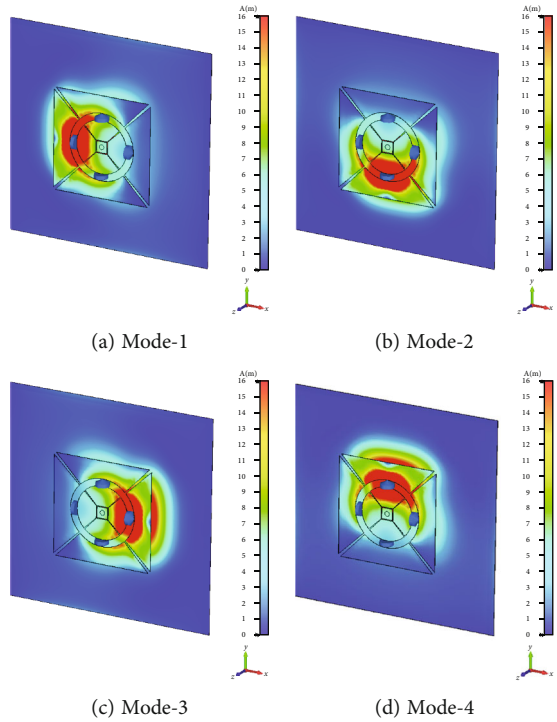

(a) Mode-1 (b) Mode-2

(c) Mode-3 (d) Mode-4

FIGURE 2: Surface current distribution of three-dimensional (3D) pattern of the single port antenna at 5.25 GHz.

for the OFF mode for simulation purposes. The bias circuit network of the proposed PRA for the PIN diode actuation has been developed according to the reference manual of the PIN diode switch. It is rather simple, as seen in Figure 1(a). Activating and deactivating the PIN diode switches enables the PRA to operate effectively in four reconfigurable modes. The switches are BAR64-02 V PIN diodes manufactured by Infineon. DC biasing lines and four radio frequency choke inductors (120 nH) are used, respectively, to limit the influence of bias current on the radiation and matching properties of the antenna and to prevent the coupling of high-frequency currents.

Table 1 indicates the relationship between switch states, reconfigurable modes, and beam direction in azimuth plane. When P_1 is connected to the power supply with Vbias = 1 V and P_2, P_3, and P_4 are connected to the ground, switch S_1 is in the ON state and the antenna operates in Mode-1. In Mode-2, P_2 is connected to the power source, while P_1, P_3, and P_4 are grounded. This indicates that switch S_2 is ON while switches S_1, S_3, and S_4 are OFF. Based on the procedure used above, Mode-3 and Mode-4 are, respectively, ON when P_3 and P_4 are connected to the power supply. As seen in Figure 2, as reconfigurable modes change, the antenna's surface current distribution shifts, causing the antenna's radiating direction to change.

2.3. PRA Performance Analysis. An antenna's performance is affected by several configuration options. The radius of the annular and the length of the trapezoid slit's bases significantly impact the proposed antenna's operating frequency. The gap between the inner and outer radius ($|R_1 - R_2|$) of the annular slit (1 mm in length for the PIN diode space) must be maintained for manufacturing simplicity and parameter manipulation. The trapezoid slit applies the same concept for adjusting the base's length. Figures 3(a) and 3(b) display the simulation of operating frequency in relation to inner radius R_1 and the base B_1 variation. When R_1 is extended from 3.75 mm to 4.25 mm in an increment of 0.125 mm, the resonance frequency lowers from 5.34 GHz to 5.61 GHz. On the other hand, the frequency resonance increases steadily as B_1 increases. $R_1 = 3.75$ mm and $B_1 = 0.07$ mm are the optimal values for the parameters with better radiation and minimized coupling. Table 2 details the optimum dimensions of the proposed PRA.

The trapezoid-shaped cells were connected by a 0.2 mm wider copper strip. The thin copper strip was removed and replaced by the PIN diode. Figure 3(c) displays the simulated (with copper strip and with PIN diode) and measured reflection coefficients (S_{11}) for optimal dimensions in Mode-1. From the standpoint of symmetry, other modes are achievable. Moreover, the measured and simulated results are highly concordant. The proposed pattern-reconfigurable square-shaped antenna operates at 5.25 GHz for four radiation modes due to its symmetrical structure. The 10 dB impedance bandwidth varies slightly between 5.163 GHz and 5.357 GHz. Figure 4 shows the four operating modes' simulated 2D radiation patterns in the azimuth plane. The main beam direction of the proposed PRA ranges from 0° to 270° in 90° increments from Mode-1 to Mode-4, respectively. Figure 4 indicates that each operating mode provides a main-beam direction and radiation pattern reconfigurability that are compatible with the proposed PRA.

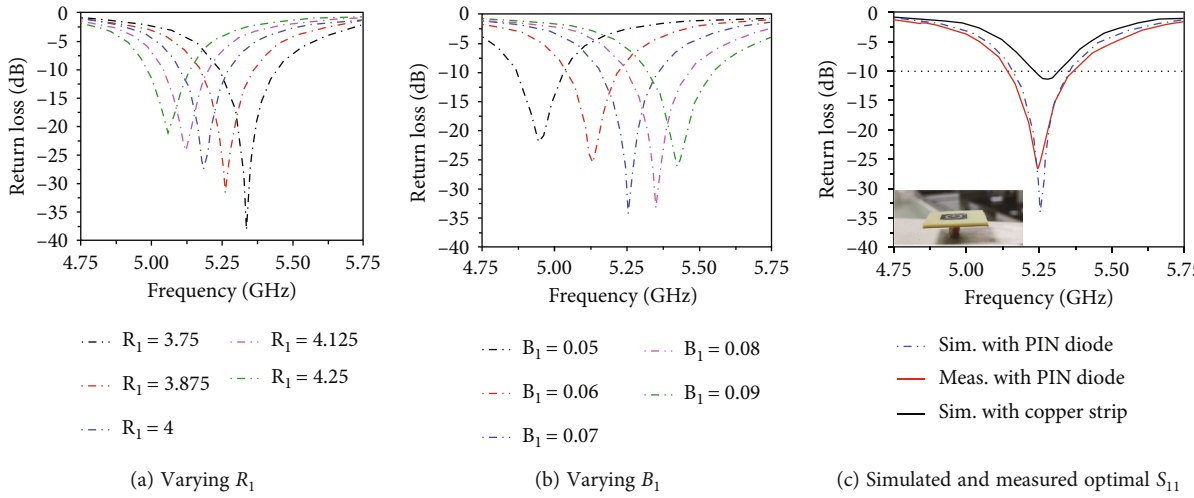

(a) Varying R_1 (b) Varying B_1 (c) Simulated and measured optimal S_{11}

FIGURE 3: The reflection coefficients of the proposed PRA for Mode-1.

TABLE 2: Optimum dimensions of the proposed PRA.

Parameters	$W = L$	W_p	B_1	B_2	R_1
Value (mm)	30	15	0.07	0.1	3.75
Parameters	L_1	L_2	L_3	h	R_2
Value(mm)	1.56	1.76	14.4	2	4.75

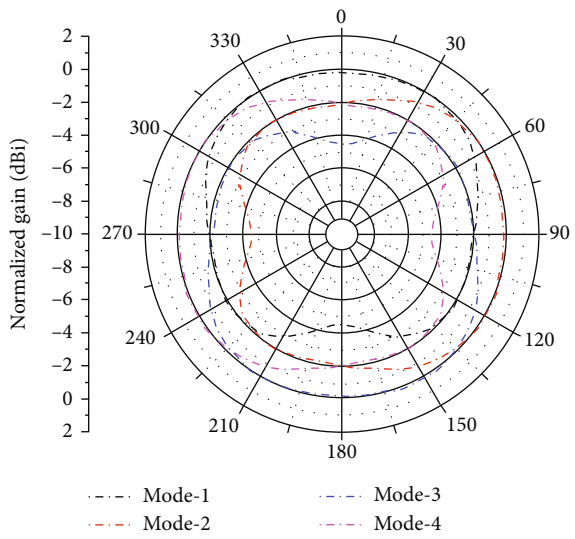

FIGURE 4: The simulated two-dimensional (2D) radiation patterns in the azimuth plane.

Except for the main beam direction in the azimuth plane, the proposed PRA's performance remains constant in all four modes. Figure 5 displays only the simulated and measured 2D radiation pattern in the azimuth plane and elevation plane for Mode-1. According to Figure 5, the radiation patterns in elevation are quite similar, and the major beam directions all point at 12°. Due to manufacturing errors and impacts from PIN diode switches and associated biasing circuit networks, slight shifts were observed. Therefore, the cross-polarizations of the radiation patterns in the elevation plane are excluded due to their insignificance. The realized gain for each of the four radiation modes is 6.25 dBi.

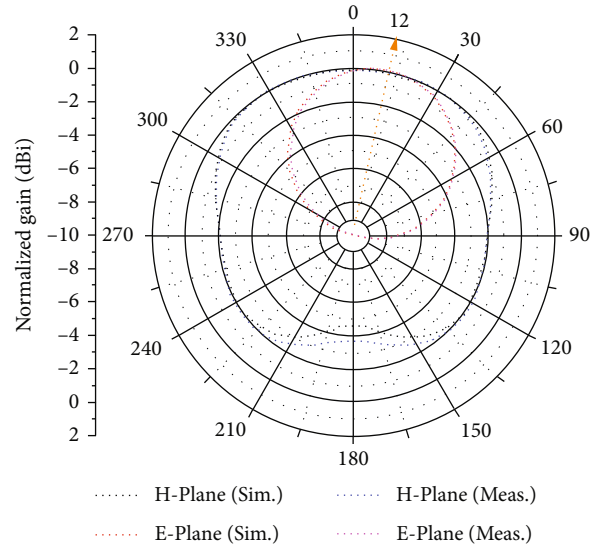

FIGURE 5: The simulated and measured 2D radiation patterns in the azimuth and elevation plane for Mode-1.

3. Wide-Angle Scanning Planar Array

3.1. Array Geometry. The proposed and manufactured scanning planar array for 5G applications is shown in Figures 6(a) and 6(b), respectively.

The proposed scanning planar array consists of 16 reconfigurable antenna elements, with the four-mode pattern each mentioned above, were grouped into four columns and four rows to form a 4×4 uniform wide-angle scanning planar array. Each PRA element has its own feeding port represented by the numbers E1, E2, E3, E4, E5…E15, and E16. The distance ($D = 0.47\lambda$) between adjacent array

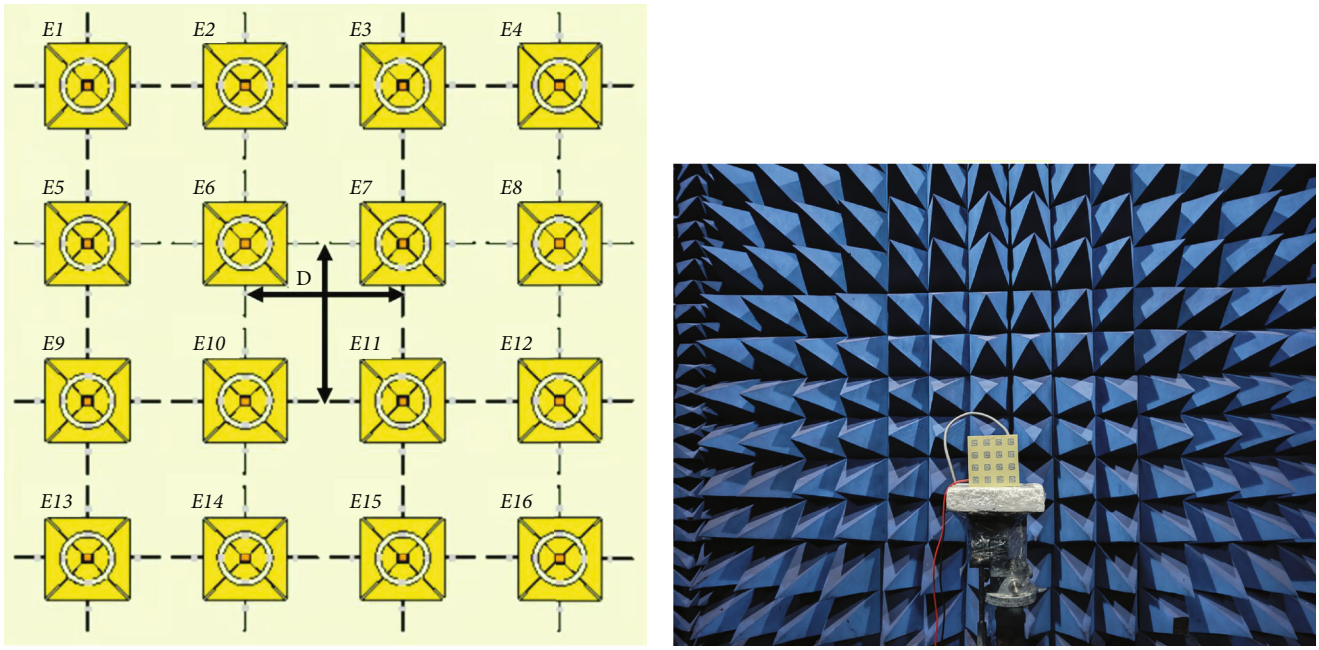

(a) (b)

FIGURE 6: (a) Geometry of the proposed scanning array. (b) Photograph of the scanning array measured in the anechoic chamber.

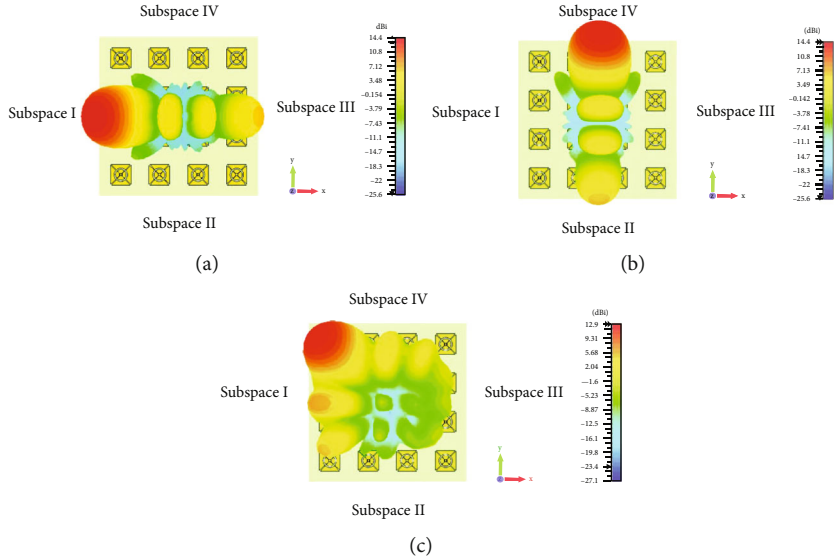

FIGURE 7: Scanning range: (a) Mode-1, $\phi_1 = 0\circ$, (b) Mode-4, $\phi_1 = 90\circ$, and (c) Mode-1 and Mode-4, $\phi_1 = 45\circ$.

elements is smaller than 0.50λ in order to prevent the grating lobes [17, 18]. The proposed 4×4 scanning planar array has overall dimensions of $1.94\lambda \times 1.94\lambda \times 0.03\lambda$. The scanning array scans the xoz plane for Mode-1 and the yoz plane for Mode-4 when port 1 of all elements is powered, as shown in Figures 7(a) and 7(b), respectively.

The active element patterns (AEPs) are employed to measure the scanning capability of the array. When one element is tested, the other elements are terminated with matching loads. The array radiation pattern may be determined as a superposition of the AEPs of all components:

$$F_{\text{array}} = \sum_{m=1}^{4}\sum_{n=1}^{4} W_{\text{mn}} f_{\text{mn}}(\theta,\varphi) e^{j\left(\text{k}\vec{\text{r}}.r_{\text{mn}} - \phi_{\text{mn}}\right)}. \quad (1)$$

Where f_{mn} represents the AEP of the $(m,n)^{\text{th}}$ element, W_{mn} and ϕ_{mn} represent the feeding amplitude and phase of the $(m,n)^{\text{th}}$ element, and r_{mn} and $\vec{r}$ are the origin-to-center position vectors of the $(m,n)^{\text{th}}$ element and the unit vector of the beam's pointing direction, respectively. Note that the feeding amplitude is equal to 1.

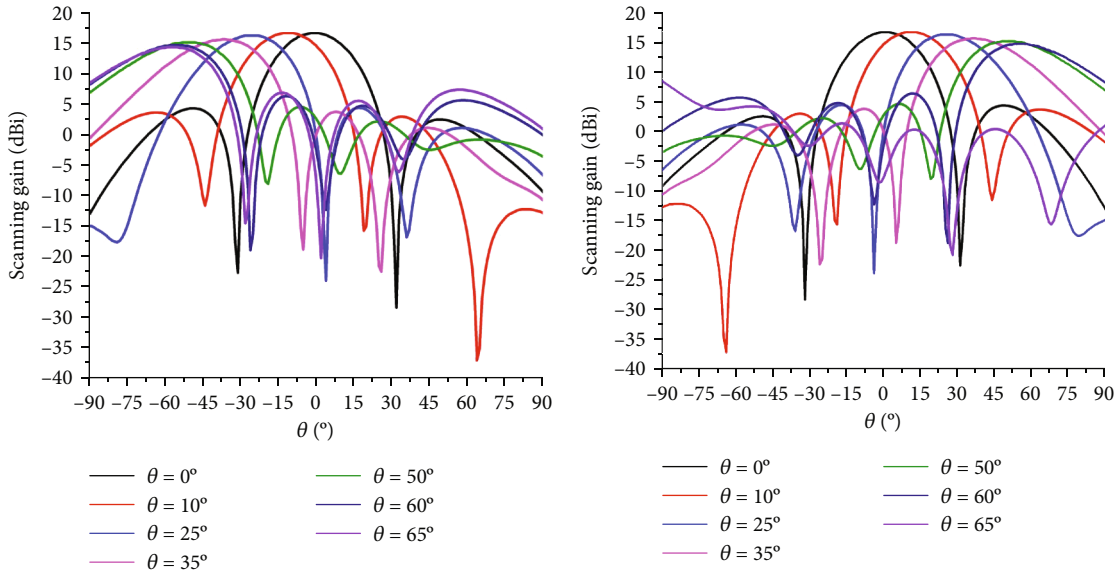

(a) Mode-1 at xoz plane

(b) Mode-4 at yoz plane

FIGURE 8: Measured scanning performance of the proposed planar array at 5.25 GHz.

TABLE 3: Performance of the scanning array with pattern reconfigurable elements.

	Scanning performance values				Plane
	$\theta_{max}(\circ)$	Gain (dBi)	MSLL (dB)	Θ_{BW}	
Mode-1 ($\phi = 0$)	0	16.6	-12.3	26.7	Xoz plane
	10	16.6	-13	26.8	
	25	16.2	-11.8	29.1	
	35	15.6	-11.8	33.6	
	50	15.1	-10.6	36.3	
	60	14.6	-8.3	36.7	
	65	14.3	-7	36.9	
Mode-4 ($\phi = 90$)	0	16.6	-12.3	26.7	Yoz plane
	10	16.6	-13	26.8	
	25	16.2	-11.8	29.1	
	35	15.6	-11.8	33.6	
	50	15.1	-10.6	36.3	
	60	14.6	-8.3	36.7	
	65	14.3	-7	36.9	

Each planar array element's pattern state is toggled by choosing the OFF/ON states of the switches. The proposed reconfigurable scanning planar array achieves 2D wide-angle beam-scanning functionality by manipulating each element's pattern state and feeding phase. To achieve wide-angle scanning in combination with pattern reconfigurability of the array, the scanning space of the array is split into four subspaces, and each subspace corresponds to one of the narrow beams (modes) of the elements. Then, after reconfigurable elements have been set to a reconfigurable mode, beam scanning in the appropriate subspace may be fine-tuned by modifying the phase shift of each element, exactly as in traditional scanning arrays [19]. The performance of the array was measured in an NSI anechoic chamber.

3.2. Array Performance Analysis. The proposed scanning planar array is designed using the four modes. Mode-1, S_1 is the only switch activated, and the feeding phase difference ϕ_1 is set to 180°. The radiation pattern of each array element is oriented to the negative x-axis, and the planar array can scan its main beam in subspace I as shown in Figure 7(a). The scanning subspace of the elements is between 13.8° and -65° in the xoz plane. Similarly, when all elements are set to Mode-3, scanning results may be obtained in the opposite subspace III (the xoz plane between -13.8° and 65°). Mode-2, S_2 is ON with the feeding phase difference ϕ_1 set to 180°, the radiation pattern of each element is slanted to the negative y-axis, and the planar array may scan its main beam in subspace II; its scanning subspace is from

Table 4: Comparison between the proposed and previous planar array.

	Reference 19	Reference 20	This work
Size (λ^3)	$2.2 \times 2.2 \times 0.17$	$1.87 \times 1.87 \times 0.09$	$1.94 \times 1.94 \times 0.03$
Scanning range (°)	[-72, 72]	[-60, 60]	[-65, 65]
Array units	4×4	4×4	4×4
Peak scanning gain (dBi)	13.6	14.8	16.6
Peak sidelobe level (dB)	5.6	4.8	7
3 dB beamwidth coverage (°)	92	80	83.5
No. of reconfigurable modes used	4	4	4
Remark	2D scanning; large size; complex control	2D scanning; compact size; complex control; low cost	2D scanning; compact size; simple control; low cost

-65° to 13.8° in the yoz plane. Similarly, when all elements are set to Mode-4, scanning results may be obtained in subspace IV (on the yoz plane between -13.8° and 65°), as shown in Figure 7(b). In Figure 7(c), by merging the scans of the subspaces, it is possible to generate a 2D simulation of a wide-angle scan of the whole 2D space by reconfiguring the pattern.

Thus, the proposed planar array's main beam can scan from -65° to 65° with side lobes less than -7 dB, and provides a 3 dB scanning coverage of up to 83.5° for in the elevation plane. Figure 8(c) illustrates the proposed array's scanning performance at 5.25 GHz for Mode-1 in the xoz plane and Figure 8(b) for Mode-4 in yoz planes. Table 3 explains Figure 8 in more depth to properly illustrate its precise details.

Due to the array's symmetry, the subspace III and VI scanning performances in Table 3 and Figure 8 are ignored. The comparison between this and other works is shown in Table 4. In addition, it demonstrates that this work has a low cost, a higher gain, broad 3-dimensional coverage, and a wide-angle scanning capability. It also has a simple design and limited mode.

4. Conclusion

Active element patterns (AEPs) are used to assess the scanning capabilities of an array. A planar array with four-mode pattern-reconfigurable elements for wide-angle scanning is made by putting the 16 PRA elements into a four-by-four grid. This proposed planar array provides broad coverage with low-side lobes. Experiments show that the main beam of the array can have a 3 dB beamwidth (BW) of more than 167° in each of the two orthogonal azimuth planes. Manufactured and analyzed, the prototype exhibited configurable beam switching capabilities, a simple design, low cost, and a simple network bias. The planar array is suitable for 5G devices.

Data Availability

Data supporting the findings of this research article are obtainable from the corresponding author upon reasonable request.

Conflicts of Interest

The authors declare that they have no conflicts of interest.

Acknowledgments

This study was supported by the National Natural Science Foundation of China, Grant numbers: 62171093 and 61731005.

References

[1] R. J. Mailloux, *Phased array antenna handbook*, Artech House, 2017.

[2] S. Hasegawa, T. Yasuzumi, Y. Kazama, and O. Hashimoto, "Phased array antenna with crossed dipole antenna for mobile satellite communications," *Microwave and Optical Technology Letters*, vol. 53, no. 12, pp. 2805–2809, 2011.

[3] S. M. Moon, S. Yun, I. B. Yom, and H. L. Lee, "Phased array shaped-beam satellite antenna with boosted-beam control," *IEEE Transactions on Antennas and Propagation*, vol. 67, no. 12, pp. 7633–7636, 2019.

[4] A. T. Muriel-Barrado, J. Calatayud-Maeso, A. Rodríguez-Gallego, P. Sánchez-Olivares, J. M. Fernández-González, and M. Sierra-Pérez, "Evaluation of a planar reconfigurable phased array antenna driven by a multi-channel beamforming module at Ka band," *IEEE Access*, vol. 9, pp. 63752–63766, 2021.

[5] H. Lago, P. J. Soh, M. F. Jamlos, and Z. Zakaria, "Beam-reconfigurable crescent array antenna with AMC plane," *International Journal of RF and Microwave Computer-Aided Engineering*, vol. 28, no. 7, article e21467, 2018.

[6] H. Zhou, A. Pal, A. Mehta et al., "Reconfigurable phased array antenna consisting of high-gain high-tilt circularly polarized four-arm curl elements for near horizon scanning satellite applications," *IEEE Antennas and Wireless Propagation Letters*, vol. 17, no. 12, pp. 2324–2328, 2018.

[7] I. E. Uchendu, J. R. Kelly, R. Mittra, and Y. Gao, "Hybrid parasitic linear array antenna for fine beamsteering applications," *IEEE Access*, vol. 9, pp. 84899–84909, 2021.

[8] M. Patriotis, F. N. Ayoub, Y. Tawk, J. Costantine, and C. G. Christodoulou, "A millimeter-wave frequency reconfigurable circularly polarized antenna array," *IEEE Open Journal of Antennas and Propagation*, vol. 2, pp. 759–766, 2021.

[9] J. A. Ganie and K. Saurav, "High gain polarization reconfigurable antenna arrays using a polarization reconfigurable converter," *International Journal of RF and Microwave Computer-Aided Engineering*, vol. 31, no. 9, article e22765, 2021.

[10] M. Li, S. Q. Xiao, and B. Z. Wang, "Investigation of using high impedance surfaces for wide-angle scanning arrays," *IEEE Transactions on Antennas and Propagation*, vol. 63, no. 7, pp. 2895–2901, 2015.

[11] R. Wang, B. Z. Wang, X. Ding, and X. S. Yang, "Planar phased array with wide-angle scanning performance based on image theory," *IEEE Transactions on Antennas and Propagation*, vol. 63, no. 9, pp. 3908–3917, 2015.

[12] Y. Q. Wen, B. Z. Wang, and X. Ding, "A wide-angle scanning and low sidelobe level microstrip phased array based on genetic algorithm optimization," *IEEE Transactions on Antennas and Propagation*, vol. 64, no. 2, pp. 805–810, 2015.

[13] Y. F. Cheng, X. Ding, W. Shao, M. X. Yu, and B. Z. Wang, "A novel wide-angle scanning phased array based on dual-mode pattern-reconfigurable elements," *IEEE Antennas and Wireless Propagation Letters*, vol. 16, pp. 396–399, 2016.

[14] B. B. Tierney, C. T. Rodenbeck, M. G. Parent, and A. P. Self, "Scalable, high-sensitivity X-band rectenna array for the demonstration of space-to-earth power beaming," *IEEE Access*, vol. 9, pp. 27897–27907, 2021.

[15] Y. F. Cheng, Z. H. Gao, L. Yang, and C. Liao, "A planar end-loaded dipole phased array with enhanced bandwidth and wide-angle scan," *International Journal of RF and Microwave Computer-Aided Engineering*, vol. 31, no. 10, article e22843, 2021.

[16] J. S. Row and J. Y. Chen, "A phased array design using a novel pattern reconfigurable antenna element," *International Journal of RF and Microwave Computer-Aided Engineering*, vol. 32, no. 8, article e23223, 2022.

[17] Z. Chen, Z. Song, H. Liu, X. Liu, J. Yu, and X. Chen, "A compact phase-controlled pattern-reconfigurable dielectric resonator antenna for passive wide-angle beam scanning," *IEEE Transactions on Antennas and Propagation*, vol. 69, no. 5, pp. 2981–2986, 2020.

[18] G. Yang and S. Zhang, "Dual polarized wide-angle scanning phased array antenna for 5G communication system," *IEEE Transactions on Antennas and Propagation*, vol. 70, no. 9, pp. 7427–7438, 2022.

[19] Y. F. Cheng, X. Ding, W. Shao, and B. Z. Wang, "Planar wide-angle scanning phased array with pattern-reconfigurable windmill-shaped loop elements," *IEEE Transactions on Antennas and Propagation*, vol. 65, no. 2, pp. 932–936, 2016.

[20] W. Zhan, S. Zhao, and D. Yuandan, "Miniaturized, vertically polarized, pattern reconfigurable dielectric resonator antenna and its phased array for wide-angle beam-steering," *IEEE Transactions on Antennas and Propagation*, vol. 70, no. 10, pp. 9233–9246, 2022.